



TITLE:

Laser induced fluorescence spectra  
of the D (1)Sigma(+)(u)-> B '  
(1)Sigma(+)(g) and C (1)Pi(g)-> A  
(1)Pi(u) systems of C-2 in solid Ne

AUTHOR(S):

Wakabayashi, T; Ong, AL; Kratschmer, W

---

CITATION:

Wakabayashi, T ...[et al]. Laser induced fluorescence spectra of the D (1)Sigma(+)(u)-> B '  
(1)Sigma(+)(g) and C (1)Pi(g)-> A (1)Pi(u) systems of C-2 in solid Ne. JOURNAL OF  
CHEMICAL PHYSICS 2002, 116(14): 5996-6001

ISSUE DATE:

2002-04-08

URL:

<http://hdl.handle.net/2433/49908>

RIGHT:

Copyright 2002 American Institute of Physics. This article may be  
downloaded for personal use only. Any other use requires prior  
permission of the author and the American Institute of Physics.

# Laser induced fluorescence spectra of the $D\ ^1\Sigma_u^+ \rightarrow B'\ ^1\Sigma_g^+$ and $C\ ^1\Pi_g \rightarrow A\ ^1\Pi_u$ systems of $C_2$ in solid Ne

Tomonari Wakabayashi<sup>a)</sup>

*Division of Chemistry, Graduate School of Science, Kyoto University, Kyoto 606-8502, Japan*

Aik-Loong Ong and Wolfgang Krätschmer

*Max-Planck-Institut für Kernphysik, Saupfercheckweg 1, D-69117 Heidelberg, Germany*

(Received 30 October 2001; accepted 15 January 2002)

In our study of carbon vapor molecules trapped in Ne matrices at 6 K, we observed laser induced fluorescence spectra of the  $D\ ^1\Sigma_u^+ \rightarrow B'\ ^1\Sigma_g^+$  system of  $C_2$  upon excitation of the Mulliken transition  $D\ ^1\Sigma_u^+ \leftarrow X\ ^1\Sigma_g^+$  of  $C_2$  at 232 nm. A vibrational progression was clearly observed going from the upper vibrational  $v'=0$  level of the electronic  $D$  state into several lower  $v''=0-6$  levels of the  $B'$  state. We found that the progression spans from 359 to 517 nm with a large Franck-Condon shift showing the intensity maximum for the 0-2 or 0-3 transition. The vibrational constants for the  $B'$  state were derived as  $\omega_e=1427\text{ cm}^{-1}$  and  $\omega_e x_e=2.1\text{ cm}^{-1}$ . We also observed the  $C \rightarrow A$  and the Swan band emissions, showing that from the excited  $D$  state also additional states were populated by internal conversion and intersystem crossing. The constants for the  $A$  state were derived as  $\omega_e=1613.5\text{ cm}^{-1}$  and  $\omega_e x_e=18.5\text{ cm}^{-1}$ . Fluorescence excitation spectra of the  $D \rightarrow B'$  vibronic transitions were found to reproduce well the relatively narrow absorption feature of the Mulliken  $D \leftarrow X$  system. We discuss the entirely different excitation spectra occurring in argon matrices in terms of matrix-site effects. Each vibronic band of the  $D \rightarrow B'$  progression shows fine structures probably due to translations and librations of  $C_2$  molecules coupled with the surrounding lattice of Ne atoms. © 2002 American Institute of Physics. [DOI: 10.1063/1.1457437]

## I. INTRODUCTION

The  $C_2$  molecule is known for its prominent emission spectra in carbon arcs, combustion flames, and atmospheric circumstances of the sun, carbon stars, and comets.<sup>1-3</sup> The rich spectroscopy of this molecule can be found in articles by Herzberg,<sup>1</sup> Weltner and Van Zee,<sup>2</sup> Van Orden and Saykally,<sup>3</sup> and Martin.<sup>4</sup> So far, more than 17 electronic states have been characterized through emission and absorption spectroscopy.<sup>2-4</sup> In earlier studies, strong emission band systems could be observed and analyzed extensively, such as in the studies of the Mulliken system in 1930's.<sup>5-8</sup> However, a series of bands, namely the LeBlanc system,<sup>9</sup> had to await understanding by laser spectroscopy until 1991.<sup>10</sup>

The lowest excited  $^1\Sigma_g^+$ -type electronic state of  $C_2$ , the  $B'$  state, had been predicted for years<sup>11-13</sup> and was finally observed in 1988 by Bernath and co-workers. Investigating microwave discharge of various hydrocarbon mixtures by a high-resolution Fourier-transform infrared (FTIR) spectrometer, these authors detected the  $B'\ ^1\Sigma_g^+ \rightarrow A\ ^1\Pi_u$  emission of  $C_2$  in the infrared.<sup>14</sup> Jackson and co-workers observed this state by recording fluorescence excitation spectra for the  $D\ ^1\Sigma_u^+ \leftarrow B'\ ^1\Sigma_g^+$  system of photofragmented acetylene.<sup>10</sup> Extending the observation to several vibronic bands, radiative lifetime of the  $B'$  state<sup>15</sup> and Franck-Condon factors for the  $D-B'$  system<sup>16</sup> have been studied in detail.

Since the optical transition between the ground-state

$X\ ^1\Sigma_g^+$  and the upper  $^1\Sigma_u^+$  level, the  $D$  state (Mulliken system), is fully allowed this transition has been investigated extensively by emission spectroscopy from a carbon arc<sup>8</sup> and recently by laser induced fluorescence (LIF) of photofragmented acetylene.<sup>17</sup>

Matrix isolation spectroscopy has been applied also to the study of  $C_2$ . Barger and Broida detected the absorption of the Swan bands of  $C_2$  in Ar, Kr, Xe,  $N_2$ ,  $CO_2$ , and  $SF_6$  matrices and the emission in a Xe matrix by electron bombardment.<sup>18</sup> Milligan *et al.* observed absorption spectra of the Mulliken system in Ar and Ne matrices by vacuum ultraviolet (UV) irradiation of acetylene in the matrix.<sup>19</sup> Frosch reported emission spectra of the Swan bands in Ar and Kr matrices by x-ray irradiation of acetylene.<sup>20</sup> Bondybey investigated the  $C_2$  relaxation dynamics in Ar and Ne matrices using sequential two-photon laser excitation of the Swan transitions, finding more than one trapping site in Ne matrices.<sup>21</sup>

Recently, parahydrogen solid and helium droplets have been used as a matrix for high-resolution spectroscopy of embedded molecules such as  $CH_4$ ,<sup>22,23</sup>  $CD_4$ ,<sup>24</sup> and  $SF_6$ ,<sup>25-27</sup> revealing reduced rotational constants compared to those in the gas phase. Linear carbon molecules  $C_n$  ( $n=3-9$ ) also were trapped in parahydrogen matrices showing fine structures in the infrared absorption spectrum.<sup>28,29</sup>

We report here on the observation of LIF spectra of the  $D \rightarrow B'$  and  $C \rightarrow A$  transitions of  $C_2$  in a solid Ne matrix. So far, such transitions have not been reported in condensed matrices.

<sup>a)</sup>A guest researcher at Max-Planck-Institut für Kernphysik. Electronic mail: waka@kuchem.kyoto-u.ac.jp

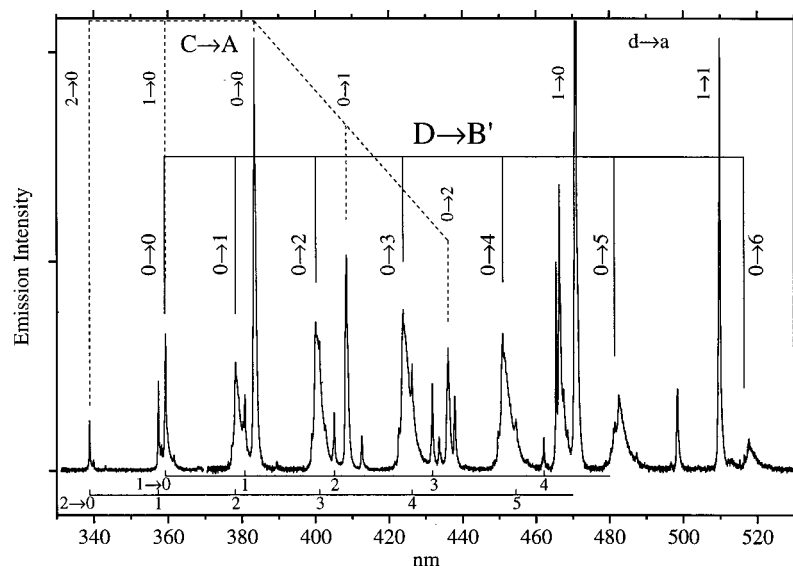


FIG. 1. Laser induced emission spectra of matrix isolated carbon molecules in solid Ne photoexcited at 232.0 nm. Observed C<sub>2</sub> emissions are the LeBlanc transitions  $D \rightarrow B'$ , Deslandres–D'Azambuja  $C \rightarrow A$ , and Swan  $d \rightarrow a$  systems. The band systems are indicated by vertical lines along with the vibrational quantum numbers of initial and final states. The vibrational progressions indicated by scales at bottom are the hot bands of the  $C \rightarrow A$  system.

## II. EXPERIMENT

The experimental setup is described elsewhere.<sup>30</sup> Briefly, carbon vapor from resistively heated graphite rods was co-condensed with an excess of neon gas on a rhodium coated sapphire substrate at 6 K. All spectra were taken in reflection. The matrix sample was irradiated with second harmonics of an excimer-pumped dye laser (Lambda Physik EMG201 MSC XeCl, FL3001 Coumarine 47 FL32 SHG). The fluorescence was collected by a lens system, dispersed by a grating monochromator (Princeton Applied Research Model 1236, 1200 G/mm,  $f=0.5$  m), and recorded on an optical multi-channel analyzer (OMA) using a time gate of a few microseconds. The detector consisted of an image-intensified charge-coupled device (ICCD) and was cooled to about  $-40$  °C by Peltier elements to reduce dark current.<sup>30</sup> Appropriate optical filters were used in order to reduce scattered laser light. The excitation and detection system was synchronized by using a delay generator operating at 30 Hz. Typical spectra were obtained by accumulating about 36 000 laser pulses. The spectral resolution was 0.2 nm. To measure the excitation function, emission spectra were recorded at various excitation wavelengths and the intensity of the considered vibronic band was plotted as a function of excitation wavelength.

## III. RESULTS

### A. LIF spectra of the $D \ ^1\Sigma_u^+ \rightarrow B' \ ^1\Sigma_g^+$ system

Figure 1 shows an emission spectrum taken at an excitation wavelength of 232.0 nm. Various band systems can be noticed. The assignments are indicated by vertical lines along with the vibrational quantum numbers for initial and final states. A distinct series of bands at 359, 378, 400, 424, 451, 482, and 517 nm was assigned to the vibrational progression ( $0 \rightarrow v''$ ;  $v''=0-6$ ) of the  $D \rightarrow B'$  system of C<sub>2</sub> with matrix shifts to the red (107–193 cm<sup>-1</sup>).<sup>16</sup> Other bands are of the  $C \rightarrow A$  (Deslandres–D'Azambuja)<sup>4,31</sup> and the  $d \rightarrow a$  (Swan)<sup>4,20</sup> systems. The progression starting at 339 nm (indicated in the bottom scale) we attribute to a progression

of the hot bands ( $2 \rightarrow v''$ ;  $v''=0-5$ ) of the  $C \rightarrow A$  system. The same progression might also be assigned to the  $C' \rightarrow A$  (Messerle–Krauss) system, in which case the 339 nm feature would be the 0–1 transition.<sup>31</sup> However, we did not observe any line which could be associated with the 0–0 transition of the  $C' \rightarrow A$  system, and therefore think that such an assignment is less likely. The linewidth for the  $C \rightarrow A$  and  $d \rightarrow a$  systems are relatively narrow, some of which are comparable to the spectral resolution, while the bands of the  $D \rightarrow B'$  system exhibit distinctly broader and structured features.

In order to compare the individual transitions, Fig. 2 shows a superposition of the members of the  $D \rightarrow B'$  system in an expanded scale given in wave numbers. For this purpose, the spectra from top to bottom (i.e., the vibronic bands of  $v'=0 \rightarrow v''=0-6$ ) were shifted in position by 27 840, 26 434, 24 998, 23 593, 22 172, 20 771, and 19 363 cm<sup>-1</sup>, respectively. In the top trace, the largest two peaks indicated by a dagger or an asterisk are mainly due to the hot bands, namely the ( $1 \rightarrow 0$ ) and ( $2 \rightarrow 1$ ) transitions of the  $C \rightarrow A$  system, respectively.<sup>31</sup> The origin band ( $0 \rightarrow 0$ ) of the  $D \rightarrow B'$  system is superposed with these peaks and not well discernible in this picture. However, from the intensity correlation at different excitation wavelengths, the bands of the  $D \rightarrow B'$  system can be clearly distinguished. A small peak at +70 cm<sup>-1</sup>, a shoulder at +10 cm<sup>-1</sup>, and a tail in between  $-20$  and  $-150$  cm<sup>-1</sup> we attribute to the origin band of the  $D \rightarrow B'$  system. In the lower traces of Fig. 2, the bands are well separated from transitions of other electronic systems. Similar fine structures are seen for the bands of 0–1, 0–2, 0–3, and 0–4; these are indicated in the second trace from top, as a main peak ‘‘a,’’ two peaks ‘‘b’’ and ‘‘c’’ at higher frequencies, and a tail ‘‘d’’ at lower frequencies. For the two traces in the bottom, i.e., the 0–5 and 0–6 transitions, the peak corresponding to the main peak ‘‘a’’ is weak compared to a broadband emerging at around  $-50$  cm<sup>-1</sup>.

A least-square fitting using the positions of the main peak ‘‘a’’ gives the vibrational frequency  $\omega_e=1427$  cm<sup>-1</sup> and the anharmonicity  $\omega_e x_e=2.1$  cm<sup>-1</sup> for the  $B'$  state in solid Ne. These constants are in good agreement with the gas

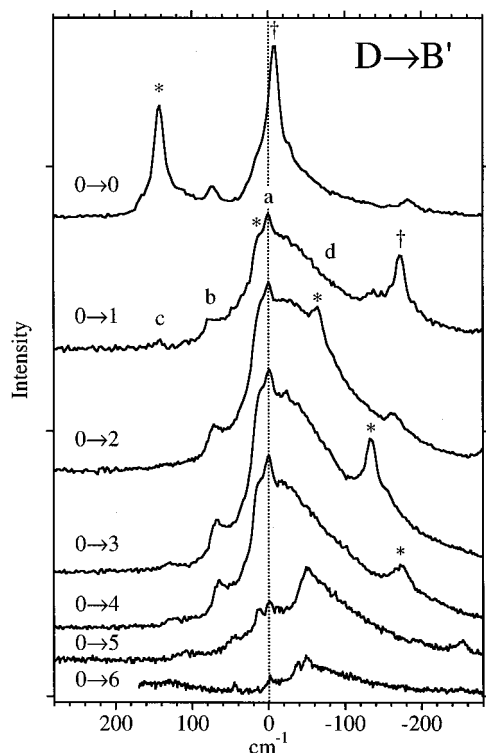


FIG. 2. Superposition of the expanded spectra (in wave numbers) of the vibronic bands ( $0 \rightarrow v''$ ;  $v'' = 0-6$ ) of the  $D \rightarrow B'$  system. The spectra from top to bottom are shifted by 27 840, 26 434, 24 998, 23 593, 22 172, 20 771, and 19 363  $\text{cm}^{-1}$ , respectively. Peaks with a dagger or an asterisk are transitions of the other electronic systems, i.e., the hot bands of the  $C \rightarrow A$  system.

phase values ( $\omega_e = 1424.1189 \text{ cm}^{-1}$  and  $\omega_e x_e = 2.57113 \text{ cm}^{-1}$ ).<sup>4,10,14,16</sup> Similarly, for the A state in solid Ne, the constants  $\omega_e = 1613.5 \text{ cm}^{-1}$  and  $\omega_e x_e = 18.5 \text{ cm}^{-1}$  are obtained in good agreement with the gas phase values ( $\omega_e = 1608.1990 \text{ cm}^{-1}$  and  $\omega_e x_e = 12.0597 \text{ cm}^{-1}$ ).<sup>4,14</sup> Table I summarizes the observed spectral positions. Table II compiles the molecular constants in Ne matrices.

A large Franck–Condon shift is noticeable for the  $D-B'$  system in Fig. 1 showing the intensity maximum for the  $0-3$  transition. It is reported from the analysis of the gas-phase spectra that the bond length in the  $B'$  state ( $r_e = 1.38 \text{ \AA}$ ) is much larger than that in the  $D$  state ( $r_e = 1.24 \text{ \AA}$ ) resulting in the maximum Franck–Condon factor for the  $0-2$  transition among the  $0-v''$  ( $v'' = 0-6$ ) transitions.<sup>16</sup> The Franck–Condon shift in Ne matrices is in good agreement with the observation in the gas phase, though the intensity of the  $0-2$  transition at  $\sim 400 \text{ nm}$  might be reduced by absorption of coexisting  $C_3$  ( $A \leftarrow X$ ) in our matrix.<sup>30</sup>

## B. Fluorescence excitation spectra

Figure 3 shows the fluorescence excitation spectra for the vibronic bands ( $0 \rightarrow v''$ ;  $v'' = 1-6$ ) of the  $D \rightarrow B'$  system (closed circles). The intensity is normalized at the peak maximum. A relatively narrow feature at  $232.0 \text{ nm}$  is characteristic for the electronic transition. The linewidth of the excitation feature is  $\sim 0.2 \text{ nm}$  ( $\sim 40 \text{ cm}^{-1}$ ). For comparison, the absorption spectra of a typical matrix sample is also

TABLE I. Peak positions of the observed LIF emission spectra of matrix isolated  $C_2$  molecules in solid Ne at  $6 \text{ K}$  upon photoexcitation at  $232.0 \text{ nm}$ . Gas-phase data are listed for comparison.

Ne <sup>a</sup> $\lambda/\text{nm}$	Gas $\lambda/\text{nm}$	Assignment	
		$v' \rightarrow v''$	Electronic system
359.2	356.728 <sup>b</sup>	0–0	$D-B'$ LeBlanc
378.3	375.769 <sup>b</sup>	0–1	
400.0	396.942 <sup>b</sup>	0–2	
423.9	420.676 <sup>b</sup>	0–3	
451.0	447.521 <sup>b</sup>	0–4	
481.5	478.194 <sup>b</sup>	0–5	
516.5	513.650 <sup>b</sup>	0–6	$C-A$ Deslandres– $D'$ Azambuja
338.8	339.07 <sup>c</sup>	2–0	
357.4	358.31 <sup>c</sup>	2–1	
359.3	360.40 <sup>c</sup>	1–0	
378.1	379.53 <sup>c</sup>	2–2	
380.8	382.22 <sup>c</sup>	1–1	
383.4	385.07 <sup>c</sup>	0–0	
401.0	403.02 <sup>c</sup>	2–3	
405.1	406.46 <sup>c</sup>	1–2	
408.4	410.08 <sup>c</sup>	0–1	
426.3	429.16 <sup>c</sup>	2–4	$d-a$ Swan
431.8	433.52 <sup>c</sup>	1–3	
436.1	438.11 <sup>c</sup>	0–2	
454.6	458.43 <sup>c</sup>	2–5	
462.2	463.92 <sup>c</sup>	1–4	
470.9	473.221 <sup>c</sup>	1–0	
509.9	512.459 <sup>c</sup>	1–1	
555.2	558.065 <sup>c</sup>	1–2	
608.7	611.706 <sup>c</sup>	1–3	

<sup>a</sup>This work in Ne matrices.

<sup>b</sup>Band positions in the gas phase from Ref. 16.

<sup>c</sup>Band positions in the gas phase calculated from molecular constants in Ref. 4.

shown in Fig. 3 (solid line). The narrow absorption feature of the Mulliken system of  $C_2$  ( $D \leftarrow X$ ) is seen at  $232.0 \text{ nm}$ <sup>19</sup> on top of the broad absorption spectrum of linear  $C_6$  spanning from  $230$  to  $240 \text{ nm}$ .<sup>32,33</sup> The sharp excitation feature of the  $D \rightarrow B'$  transition coincides with the sharp absorption feature of the  $D \leftarrow X$  transition of  $C_2$ .

The excitation spectrum for the  $C \rightarrow A$  transitions is also shown in Fig. 3 (open circles). This spectrum shows a broad feature centered at  $233.5 \text{ nm}$ , i.e., shifted by  $1.5 \text{ nm}$  from the absorption maximum at  $232.0 \text{ nm}$ . The absorption feature

TABLE II. Constants in wavenumbers of  $C_2$  electronic states involved in this work in neon matrices. Numbers in parentheses are the corresponding gas phase values taken from Ref. 4.

Electronic state	Solid Ne		
	$T_e$	$\omega_e$	$\omega_e x_e$
$D \ ^1\Sigma_u^+$	43 103 <sup>a</sup> (43 239.4)	...	(1829.6)
$C \ ^1\Pi_g$	...	1784 <sup>c</sup> (1809.1)	34.1 <sup>c</sup> (15.8)
$B' \ ^1\Sigma_g^+$	15 264 <sup>b</sup> (15 409.1)	1427 <sup>d</sup> (1424.1)	2.1 <sup>d</sup> (2.6)
$A \ ^1\Pi_u$	...	1613.5 <sup>e</sup> (1608.2)	18.5 <sup>e</sup> (12.1)
$X \ ^1\Sigma_g^+$	0	...	(1855.0)

<sup>a</sup> $\nu_{00}(D-X)$  in  $\text{cm}^{-1}$ .

<sup>b</sup>Difference frequency  $\nu_{00}(D-X) - \nu_{00}(D-B')$ .

<sup>c</sup>Quadratic fitting of  $C-A(v' \rightarrow 0; v'' = 0-2)$ .

<sup>d</sup>Quadratic fitting of  $D-B'(0 \rightarrow v''; v'' = 0-6)$ .

<sup>e</sup>Quadratic fitting of  $C-A(0 \rightarrow v''; v'' = 0-2)$ .

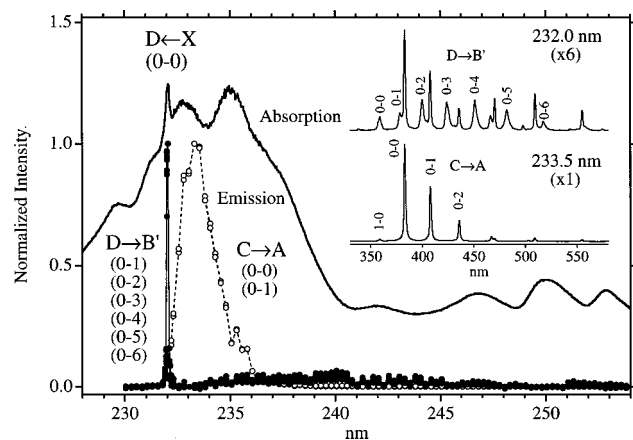


FIG. 3. Fluorescence excitation spectra for selected vibronic transitions of the  $D \rightarrow B'$  (closed circles) and the  $C \rightarrow A$  (open circles) systems. The emissions are scaled to the maximum. For comparison, a typical absorption spectrum (solid line) of the matrix sample is shown. The background absorption originates from larger clusters  $C_n$  which are trapped in the matrix together with  $C_2$ . Inset shows fluorescence emission spectra excited at 232.0 nm (upper panel) and at 233.5 nm (lower panel).

corresponding to the excitation curve for the  $C \rightarrow A$  transitions is very weak and difficult to discern, whereas the intensity of the LIF signal of the  $C \rightarrow A$  transitions at the intensity maximum at 233.5 nm is about ten times higher than that for  $D \rightarrow B'$  at 232.0 nm.

The inset in Fig. 3 compares the fluorescence spectra of on- and off-resonant excitations to the  $D \leftarrow X$  transition; the spectra for the excitation wavelength at 232.0 nm (upper panel) which corresponds to the intensity maximum of the  $D \rightarrow B'$  emissions and at 233.5 nm (lower panel) for which the bands of the  $C \rightarrow A$  transitions are observed almost exclusively.

## IV. DISCUSSION

### A. The electronic configuration of free $C_2$

The  $C_2$  molecule has  $D_{\infty h}$  point group symmetry. The electronic ground-state configuration  $(2\sigma_g)^2(2\sigma_u)^2(1\pi_u)^4$

yields a singlet  $^1\Sigma_g^+$  state.<sup>4,13</sup> The  $B'$  and a higher lying  $E$  state have the same symmetry but arise from different configurations, namely of  $(2\sigma_g)^2(2\sigma_u)^2(1\pi_u)^2(3\sigma_g)^2$  and  $(2\sigma_g)^2(2\sigma_u)^0(1\pi_u)^4(3\sigma_g)^2$ , respectively. Both are doubly excited configurations. The  $D$  state corresponds to the configuration  $(2\sigma_g)^2(2\sigma_u)^1(1\pi_u)^4(3\sigma_g)^1$  and possesses  $^1\Sigma_u^+$  symmetry. In the  $D \leftarrow X$  transition, one  $2\sigma_u$  electron is excited to the  $3\sigma_g$  state, a process which satisfies the optical selection rules ( $g \leftrightarrow u$  and  $\Delta\Lambda = 0$ ), and thus this transition is fully allowed. On the other hand, in the  $D \rightarrow B'$  transition, two  $1\pi_u$  electrons move simultaneously, one down to the  $2\sigma_u$  level and the other up to the  $3\sigma_g$  level. Earlier theoretical work has shown that such double-excitation processes are optically forbidden.<sup>34</sup> However, using multireference configuration interaction (MRDCI) method, Bruna and Wright recently suggested that the  $D \leftrightarrow B'$  transition ( $1\pi_u 1\pi_u \leftrightarrow 2\sigma_u 3\sigma_g$ ) might “borrow” intensity from the allowed transitions  $D \leftrightarrow X$  and  $E \leftrightarrow D$  ( $2\sigma_u \leftrightarrow 3\sigma_g$ ) through configurational mixing of  $B'$ ,  $X$ , and  $E$ , since all these states have the same  $^1\Sigma_g^+$  symmetry.<sup>35</sup> According to these authors, the  $E$  character in  $B'$  increases with decreasing bond length. As a result, the transition intensity of the  $D \rightarrow B'$  system increases steeply with decreasing bond length.

Figure 4 illustrates the electronic and some vibrational energy levels of  $C_2$  reproduced from gas-phase molecular constants in the literature.<sup>4</sup> Obviously, the  $D \rightarrow B'$  transitions originate from direct relaxation from the  $D$  state to which the molecules are photoexcited (see vertical lines from the uppermost  $D$  level in Fig. 4). The resemblance of the fluorescence excitation curve with the absorption feature at 232.0 nm in Fig. 3 supports this idea. Note that other relaxation channels should also contribute to some extent. The intensity of the LIF signals of the  $d \rightarrow a$  transitions observed at 471, 510, 555, and 609 nm is well correlated with that of the  $D \rightarrow B'$  transitions. The former are decay channels into triplet spin states via intersystem crossing, suggesting strong spin-orbit coupling or significant configurational mixing of triplet and singlet states.

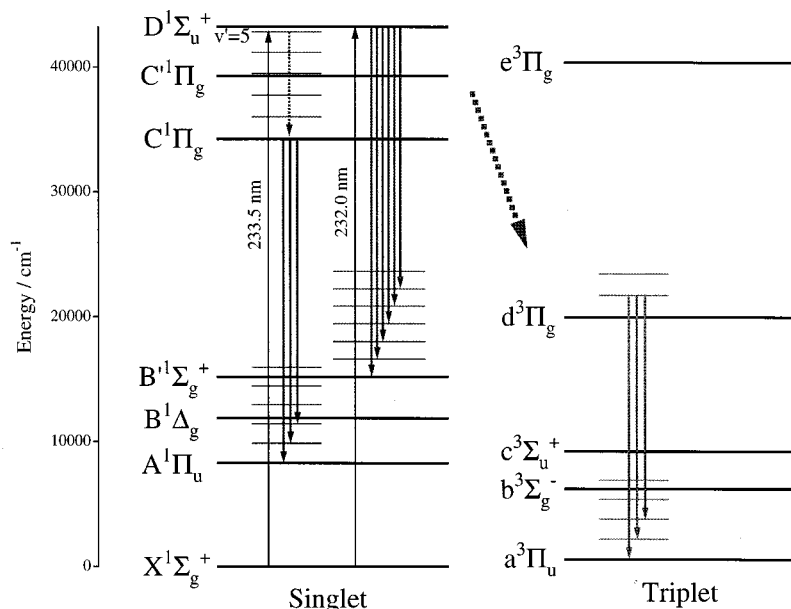


FIG. 4. Electronic and some vibrational energy levels of  $C_2$ . The state labeled  $E$  ( $^1\Sigma_g^+$ ) and further states at higher energy are not shown. The vibronic data are taken from Ref. 4.



## B. Comparison between excitation curves for $D \rightarrow B'$ and $C \rightarrow A$

The fluorescence excitation curve of the  $C \rightarrow A$  transitions (in Fig. 3, open circles) is in position and width qualitatively different from that of the  $D \rightarrow B'$  transition. The intensity maximum is located at 233.5 nm, i.e., shifted by about  $280\text{ cm}^{-1}$  lower in energy compared to the maximum of  $D \rightarrow B'$ . The width of the excitation feature is roughly  $400\text{ cm}^{-1}$  which is one order of magnitude broader than that for  $D \rightarrow B'$ . One might consider that, when the phonons are excited simultaneously with the electronic excitation, the relaxation of the upper  $D$  state may proceed more efficiently to exhibit the fluorescence decay exclusively from the lower  $C$  state.<sup>36,37</sup> However, the excitation energy in the present case is apparently lower even than the energy of the zero phonon excitation of the  $D \leftarrow X$  transition. Here the question arises how the  $C$  system can be reached from the ground state and to which vibronic state of the  $C$  system the molecule has to be excited to explain the fluorescence decay via  $C \rightarrow A$ .

In the gas phase, the transition between  $C\ ^1\Pi_g$  and  $X\ ^1\Sigma_g^+$  is strictly forbidden because both have *gerade* electronic wave functions in  $D_{\infty h}$ . In the matrix, however, also the crystal field in which the  $C_2$  molecule is embedded has to be taken into account. The  $C_2$  molecule, e.g., may translate back and forth and/or liberate around a lattice point. As a result, in some moments, the molecule may be located at a symmetric position in the crystal field where the molecular symmetry is retained and only intrinsically allowed transition of  $D \leftarrow X$  occurs like in the gas phase. Then, in another moment, the  $C_2$  molecule may reach an asymmetric position where the overall symmetry is reduced and the forbidden transition becomes allowed. In Fig. 4, we suppose that an upper level of  $v' = 5$  of the  $C$  state is located slightly below the vibrationally ground level of the  $D$  state. By intensity "borrowing" from the fully allowed  $D \leftarrow X$  transition, the  $C \leftarrow X$  transition should occur via the vibronic ( $5 \leftarrow 0$ ) level. Efficient internal conversion from  $v = 5$  to  $v = 0$  within the  $C$  state may lead to the exclusive fluorescence decay channel via  $C \rightarrow A$  transitions.

Concerning the width of the excitation curve for  $C \rightarrow A$  transitions, we should note the observation that in argon matrices the excitation spectrum shows a broad feature similar to that in Ne matrices, though red-shifted to 238 nm.<sup>38</sup> This excitation spectrum in Ar (not shown)<sup>38</sup> resembles a relatively broad absorption feature at 238 nm with a bandwidth of  $\sim 400\text{ cm}^{-1}$ .<sup>19</sup> Upon photoexcitation of this broad absorption feature in Ar matrices, only  $C \rightarrow A$  transitions and relatively weak Swan transitions can be observed in LIF spectra. Any trace of  $D \rightarrow B'$  transitions is not observed in Ar matrices. Furthermore, no sharp absorption feature which might give  $D \rightarrow B'$  transitions was observed in Ar.<sup>38</sup> Thus, we conclude that in Ar matrices the  $C_2$  molecules are exclusively trapped in *asymmetric* sites exhibiting a broad UV absorption feature and a corresponding broad excitation curve for  $C \rightarrow A$  transitions. On the other hand, in Ne matrices,  $C_2$  molecules are located in both, *asymmetric* and *symmetric* sites. Only in the latter case, the sharp absorption feature of the  $D \leftarrow X$  system and the fluorescence decay via  $D \rightarrow B'$  transitions are observed.

## C. Fine structures in $D \rightarrow B'$ system

Fine structures observed in the  $D \rightarrow B'$  fluorescence spectra (see Fig. 2) are attributable to librational and translational motions of  $C_2$  coupled with phonons of the Ne lattice. The separations of peaks "b," "c," and "d" measured from the main peak "a" in Fig. 2 being  $10\text{--}150\text{ cm}^{-1}$  are orders of magnitude larger than those expected for free rotation of  $C_2$  ( $B_e = 1.481\text{ cm}^{-1}$  for the  $B'$  state in the gas phase).<sup>4,14</sup> One might consider hot bands of the  $D \rightarrow B'$  system, i.e.,  $1\text{--}0, 1\text{--}1, \dots, 2\text{--}0, 2\text{--}1, \dots$ , and so on. However, in low temperature matrices and at a slow repetition rate of the pulsed-laser excitation, most excited molecules are quenched to the ground-state  $X$  ( $v = 0$ ) before the next laser pulse. Thus, the population in  $v \geq 1$  levels in the  $D$  state should be negligible. We observed no candidate for a hot band in the  $D \rightarrow B'$  progression (see Fig. 1).

As is apparent from the large Franck-Condon shift for the  $D \leftarrow B'$  transitions in Fig. 1, the difference in bond length between  $D \leftarrow B'$  systems is larger than that for  $C \leftarrow A$ ,  $d \leftarrow a$ , and  $D \leftarrow X$  systems. Using the gas-phase constants,<sup>4</sup> the difference  $\Delta r_e/r_e$  is calculated as  $+11.3\%$  for  $D \rightarrow B'$ ,  $+5.3\%$  for  $C \rightarrow A$ ,  $+2.9\%$  for  $C' \rightarrow A$ ,  $+3.6\%$  for  $d \rightarrow a$ , and  $-0.6\%$  for  $D \leftarrow X$ . As a result of the relatively large extension of the C-C bond length upon  $D \rightarrow B'$  transitions, phonons of the Ne lattice can be easily excited giving rise to the structured spectra as in Figs. 1 and 2.

We believe that the observed fine structures are due to librations and translations of  $C_2$  molecules in the excited  $B'$  state. Our preliminary calculations in which we for simplicity considered a cluster consisting of a single  $C_2$  molecule trapped in mono-substitutional site of a close-packed face-centered-cubic (fcc) crystal of 12 surrounding Ne atoms shows that the interaction energy between  $C_2$  and Ne is of the order of a few tens of wave numbers. For the electronic ground state, a lot of librational and translational motions are found in the energy range well below  $150\text{ cm}^{-1}$ .<sup>39,40</sup> These motions may be regarded as vibrational modes of a cluster  $C_2\text{Ne}_x$ , in which a  $C_2$  molecule is surrounded by  $x$  Ne atoms in a fcc fashion. Some modes are coupled with rotations of  $C_2$  (librations), some with translations back and forth, and the rest are vibrations solely of Ne atoms, depending on the vibrational symmetry of the cluster  $C_2\text{Ne}_x$  considered. Phonon frequencies of pure Ne crystals are also of similar order or lower, i.e., in between  $0\text{--}60\text{ cm}^{-1}$ .<sup>41,42</sup> It might be interesting to extend such calculations to vibrational modes for bulk systems of solid Ne containing small amount of  $C_2$  molecules as impurities, using appropriate periodic boundary conditions. This kind of approach would give a microscopic picture of molecular motions in a weakly bound low temperature crystal.

## ACKNOWLEDGMENTS

We thank Professor William M. Jackson and Professor Takeshi Oka for the historical view on spectroscopy of  $C_2$ . Professor Kensuke Harada is acknowledged for the discussion on van der Waals complexes. T.W. was supported by the MPI für Kernphysik international collaboration program in 2000 and 2001. This work is supported in part by The Grant

in Aid from The Ministry of Education, Science, Sports, and Culture of Japan and by a project in CREST of Japan Science and Technology Corporation.

- <sup>1</sup>G. Herzberg, *Molecular Spectra and Molecular Structure I, Spectra of Diatomic Molecules*, D. Van Nostrand Company (Canada) Ltd. (1950).
- <sup>2</sup>W. Weltner, Jr. and R. J. Van Zee, *Chem. Rev.* **89**, 1713 (1989).
- <sup>3</sup>A. Van Orden and R. J. Saykally, *Chem. Rev.* **98**, 2313 (1998).
- <sup>4</sup>M. Martin, *J. Photochem. Photobiol., A* **66**, 263 (1992).
- <sup>5</sup>R. S. Mulliken, *Z. Elektrochem.* **36**, 603 (1930).
- <sup>6</sup>T. Hori, *Z. Phys.* **88**, 495 (1934).
- <sup>7</sup>J. G. Fox and G. Herzberg, *Phys. Rev.* **52**, 638 (1937).
- <sup>8</sup>O. G. Landsverk, *Phys. Rev.* **56**, 769 (1939).
- <sup>9</sup>O. Sorkhabi, V. M. Blunt, H. Lin, D. Xu, J. Wrobel, R. Price, and W. M. Jackson, *J. Chem. Phys.* **107**, 9842 (1997).
- <sup>10</sup>Y. Bao, R. S. Urdahl, and W. M. Jackson, *J. Chem. Phys.* **94**, 808 (1991).
- <sup>11</sup>P. F. Fongere and R. K. Nesbet, *J. Chem. Phys.* **44**, 285 (1966).
- <sup>12</sup>J. Barsuhn, *Z. Naturforsch. A* **27**, 1031 (1972).
- <sup>13</sup>K. Kirby and B. Liu, *J. Chem. Phys.* **70**, 893 (1979).
- <sup>14</sup>M. Douay, R. Nietmann, and P. F. Bernath, *J. Mol. Spectrosc.* **131**, 261 (1988).
- <sup>15</sup>M. Gong, Y. Bao, R. S. Urdahl, and W. M. Jackson, *Chem. Phys. Lett.* **217**, 210 (1994).
- <sup>16</sup>O. Sorkhabi, D. D. Xu, V. M. Blunt, H. Lin, R. Price, J. D. Wrobel, and W. M. Jackson, *J. Mol. Spectrosc.* **188**, 200 (1998).
- <sup>17</sup>V. M. Blunt, H. Lin, O. Sorkhabi, and W. M. Jackson, *J. Mol. Spectrosc.* **174**, 274 (1995).
- <sup>18</sup>R. L. Burger and H. P. Broida, *J. Chem. Phys.* **43**, 2371 (1965).
- <sup>19</sup>D. E. Milligan, M. E. Jacox, and L. Abouaf-Marguin, *J. Chem. Phys.* **46**, 4562 (1967).
- <sup>20</sup>R. P. Frosch, *J. Chem. Phys.* **54**, 2660 (1971).
- <sup>21</sup>V. E. Bondybey, *J. Chem. Phys.* **65**, 2296 (1976).
- <sup>22</sup>S. Tam, M. E. Fajardo, H. Katsuki, H. Hoshina, T. Wakabayashi, and T. Momose, *J. Chem. Phys.* **111**, 4191 (1999).
- <sup>23</sup>T. Momose, M. Miki, T. Wakabayashi, T. Shida, M.-C. Chan, S. S. Lee, and T. Oka, *J. Chem. Phys.* **107**, 7707 (1997).
- <sup>24</sup>H. Hoshina, T. Wakabayashi, T. Momose, and T. Shida, *J. Chem. Phys.* **110**, 5728 (1999).
- <sup>25</sup>M. Hartmann, R. E. Miller, J. P. Toennies, and A. Vilesov, *Phys. Rev. Lett.* **75**, 1566 (1995).
- <sup>26</sup>J. Harms, M. Hartmann, J. P. Toennies, A. F. Vilesov, and B. Sartakov, *J. Mol. Spectrosc.* **185**, 204 (1997).
- <sup>27</sup>H. Katsuki, T. Momose, and T. Shida *J. Chem. Phys.* (submitted).
- <sup>28</sup>S. Tan, M. MacIer, and M. Fajardo, *J. Chem. Phys.* **106**, 8955 (1997).
- <sup>29</sup>M. Miki, T. Wakabayashi, T. Momose, and T. Shida, *J. Phys. Chem.* **100**, 12135 (1996).
- <sup>30</sup>I. Černák, M. Förderer, I. Čermáková, S. Kalhofer, H. Stopka-Ebeler, G. Monninger, and W. Krätschmer, *J. Chem. Phys.* **108**, 10129 (1998).
- <sup>31</sup>G. Messerle and L. Krauss, *Z. Naturforsch. A* **22**, 2015 (1967).
- <sup>32</sup>M. Grutter, M. Wyss, E. Riaplov, J. P. Maier, S. D. Peyerimhoff, and M. Hanrath, *J. Chem. Phys.* **111**, 7397 (1999).
- <sup>33</sup>T. Wakabayashi, A.-L. Ong, and W. Krätschmer, "Laser Induced Dissociation of Linear C<sub>6</sub> and Reorientation of Trapping Sites in Solid Neon," in *AIP Conference Proceedings 590, Nanonetwork Materials: Fullerenes, Nanotubes, and Related Systems; ISNM 2001*, edited by S. Saito *et al.* (2001), pp. 513–516.
- <sup>34</sup>H. H. Jaffe and M. Orchin, *Theory and Application of Ultraviolet Spectroscopy* (Wiley, New York, 1962).
- <sup>35</sup>P. J. Bruna and J. S. Wright, *J. Phys. Chem.* **96**, 1630 (1992).
- <sup>36</sup>V. E. Bondybey and J. H. English, *Chem. Phys. Lett.* **60**, 69 (1978).
- <sup>37</sup>V. E. Bondybey and J. H. English, *J. Chem. Phys.* **72**, 3113 (1980).
- <sup>38</sup>T. Wakabayashi, A.-L. Ong, and W. Krätschmer (unpublished).
- <sup>39</sup>The vibrational modes of C<sub>2</sub>Ne<sub>12</sub> clusters with *D*<sub>4h</sub> and *D*<sub>3d</sub> point group symmetries were derived using GAUSSIAN 98 (Ref. 40) at the B3LYP/cc-pVDZ level of theory, where the positions of 13 Ne atoms were fixed to those corresponding to pure crystal of Ne in a face-centered-cubic (fcc) structure and the central Ne atom was replaced with a C<sub>2</sub> molecule such that the molecular axis was located along a *C*<sub>4</sub> axis of the Ne<sub>12</sub> cluster for the former and a *C*<sub>3</sub> axis for the latter.
- <sup>40</sup>M. J. Frisch, G. W. Trucks, H. B. Schlegel *et al.*, GAUSSIAN 98, Revision A.9, Gaussian, Inc., Pittsburgh, PA, 1998.
- <sup>41</sup>M. L. Klein and T. R. Koehler, "Lattice Dynamics of Rare Gas Solids," in *Rare Gas Solids I*, edited by M. L. Klein and J. A. Venables (Academic, London, 1976), pp. 301–381.
- <sup>42</sup>H. J. Jodl, "Solid-State Aspects of Matrices," in *Chemistry and Physics of Matrix-Isolated Species*, edited by L. Andrews and M. Moskovits (Elsevier, Amsterdam, 1989), pp. 343–415.